# 3D-QSAR Model for GyrB ATPase Inhibition of *E.Coli* by Small Molecules

Pia Schieback and Thomas Lemcke
*University of Hamburg, Institute of Pharmacy, Bundesstr. 45, D-20146 Hamburg, Germany*

## Introduction

DNA gyrase is one of the most important targets for antibacterial agents and gyrase inhibitory compounds are widely used to treat bacterial infections [1]. The increasing use of broad-spectrum antibacterial compounds such as fluoroquinolones, which inhibit gyrase subunit A, beta-lactam antibiotics, or sulfonamides, led to the development of multi-drug resistant pathogens. Therefor inhibition of DNA gyrase subunit B through active antibacterial agents got more attention as a clinical useful target against such bacteria ( i.e. Escherichia coli) with multi-drug resistant strains. The advantage of this target is that it only exists in bacteria (like gyrA) and not in human cells and the high degree of sequence conservation in many bacterial species [2]. Novobiocin, an aminocoumarine derivate, was used to inhibit the ATPase domain of the gyrase subunit B, but it was unsuccessful in clinical therapy because of serious side effects. Currently there are no antibacterial agents which inhibit gyrB used for antibacterial therapy[3]. In connection with a project to identify new small molecule inhibitors of the ATPase of the gyrB subunit of bacterial gyrase, 3D-QSAR models for the inhibition of E. coli gyrB ATPase by a set of structurally diverse small molecules were generated.

## Methods

### Structure alignment

143 structures with known gyrB inhibitory activity data (87 with $IC_{50}$- and 56 with $K_D$-values) were collected from the literature. All compounds were docked to the ATP-binding sites of 4 gyrB x-ray crystal structures (PDB-code: 1EI1 [4], 1AJ6 [5], 3G7E [6] and 4DUH [7]) using the SP-mode of GLIDE from the Schrödinger Molecular Modeling Suite [8]. One docking pose for each compound was selected after visual inspection (selection criteria: accordance with literature data, hydrogen bond (HB) to asp73, a conserved water molecule and arg136 (figure 1), high docking score). The resulting "docked-alignment" is shown in figure 2.

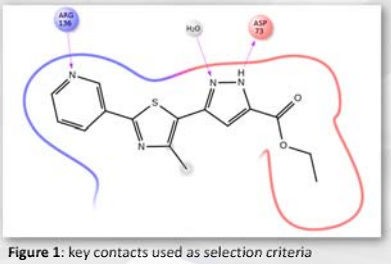


**Figure 1**: key contacts used as selection criteria during the extraction of docking poses

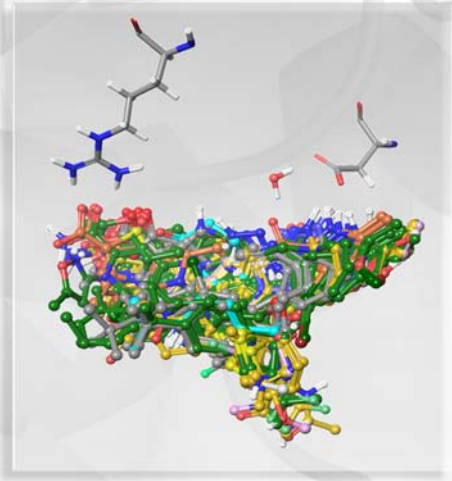

**Figure 2**: Docked-Alignment of 87 compounds with known $IC_{50}$ data. Important binding site residues Asp73 and Arg136 and structural water are also depicted.

### CoMSIA (Comperative Molecular Similarity Indices Analysis)

AM1 charges were calculated for all compounds using MOPAC [9]. The two data sets were split into a trainings and a test set by randomly selecting 25 % of the compounds respectively for test sets. CoMSIA fields (steric, electrostatic, hydrophobic, HB-donor, HB-acceptor) were calculated using the default parameters by the advanced QSAR module of Sybyl X 2.1 [10].
Leave-One-Out (LOO) crossvalidated PLS (Partial Least Squares) analysis were performed using all possible field combinations for both trainihng sets. Non crossvalidated full pls-models were subsequently calcuated for the field combinations showing the best $Q^2$-values. The best perfoming CoMSIA models were used finally used to predict the activity ($IC_{50}$ or $K_D$) of the test set compounds.

## Results

| | $K_D$ Model | $IC_{50}$ Model |
|---|---|---|
| statistics of models | | |
| $Q^2$ | 0.92 | 0.644 |
| Standard Error of Estimate | 0.128 | 0.516 |
| $R^2$ | 0.997 | 0.84 |
| Standard Deviation | 0.662 | 0.771 |
| F | 1626.788 | 107.142 |
| Components | 7 | 3 |
| $R^2$ of test set | 0.7956 | 0.5691 |
| field distribution | | |
| Steric | 18,4% | - |
| Electrostatic | 26,4% | 40,9% |
| Hydrophobic | 26,6% | 34,4% |
| Donor | - | 24,7% |
| Acceptor | 28,6% | - |

**Table 1**: Evaluation of the models

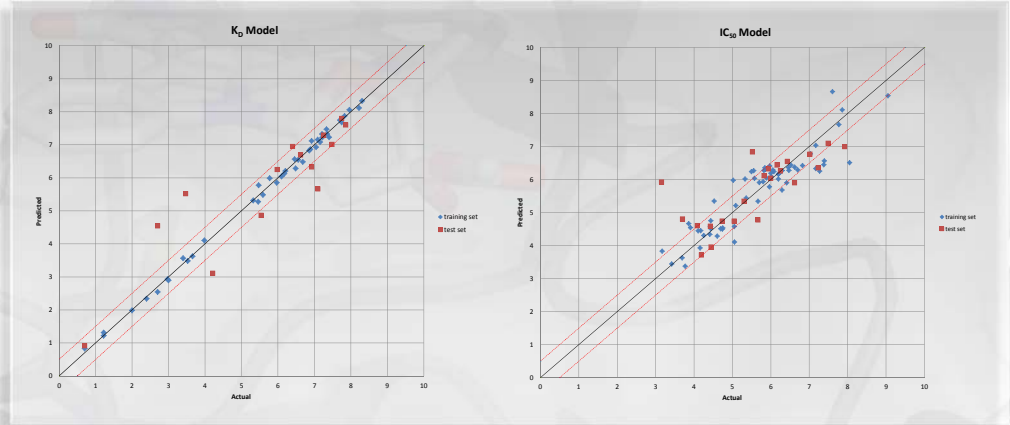


**Figure 3**: Plot of experimental activity ($pIC_{50}$/$pK_D$) against predicted activity by the best CoMSIA models.

The data for the best $K_D$ and $IC_{50}$ model are given in Table 1. While both models show good internal predictivity ($Q^2$), the $K_D$ model performs much better. This is illustrated by the plot in figure 3. All compounds of the trainings set are predicted within less than half a log unit of the actual activity. The test set is predicted quite well by both models, but some compounds are still overpredicted by more than 1 log unit. This might be due to special structural features of the given compounds, that are not well represented in the trainings set. Figures 4a/b show the electrostatic (4a) and steric (4b) contour maps from the $K_D$ CoMSIA Model, together with either a very active compound or with a less active training compound. This proves the usefulness of the models for interpretation of structure – activity relationships.

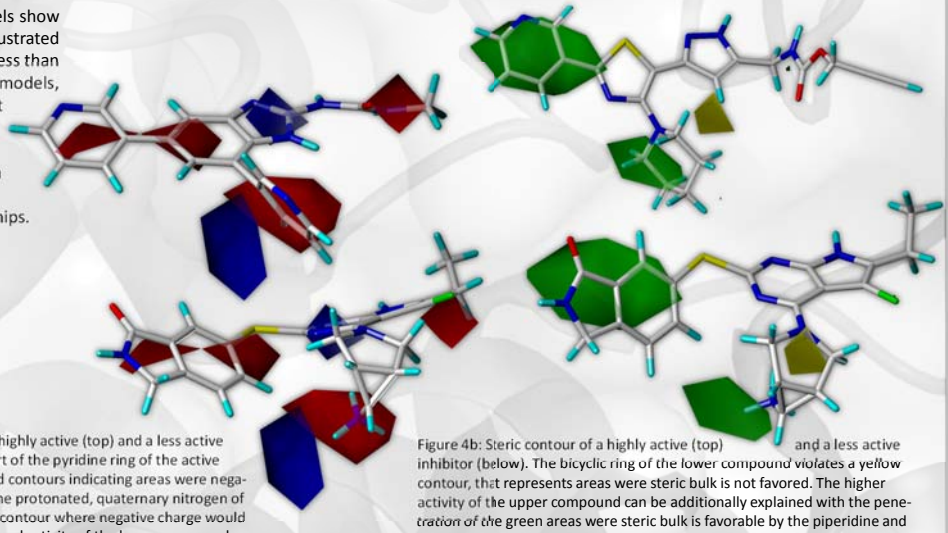

Figure 4a: Electrostatic contour of a highly active (top) and a less active inhibitor (below). The amide and part of the pyridine ring of the active compound penetrate the red colored contours indicating areas were negatively charged groups are favored. The protonated, quaternary nitrogen of the lower compound is also inside a contour where negative charge would be favorable. This results in a decreased activity of the lower compound.

Figure 4b: Steric contour of a highly active (top) and a less active inhibitor (below). The bicyclic ring of the lower compound violates a yellow contour, that represents areas were steric bulk is not favored. The higher activity of the upper compound can be additionally explained with the penetration of the green areas were steric bulk is favorable by the piperidine and pyridine ring system.

## Conclusion

A docking based alignment that used information from known protein-ligand com-plexes led statistical significant CoMSIA models. The model based on $K_D$ data per-formed better than the respective $IC_{50}$ model, both in terms of internal and external predictivity. Analysis and interpretation of the contour maps from the different CoMSIA fields will aid the design process of new gyrB inhibitors.
The generated 3D-QSAR models will be used to score potential hits in an ongoing virtual screening campaign for new and selective gyrB inhibitors.

## References

1. Nakaminami, H.; Sato-Nakaminami, K.; Noguchi, N. (2014). Int. J. Antimic. Ag.: 43(5): 478-479
2. Tari, L.W.;Trzoss, M.; Bensen, D. C.; Li, X.; Chen, Z.; Lam, T.; Zhang, J.; Creighton, C. J.; Cunningham, M. L.; Kwana, B.; Stidham, M.; Shaw, K. J.; Lightstone, F.C.; Wongb, S. E.; Nguyen, T.B.; Nix, J.; Finn, J. (2013). Bioorg. Med. Chem. Lett.: 23(5): 1529-1536
3. Collin, F.; Karkare, S., Maxwell, A. (2011). Appl. Microbiol. Biotechnol.: 479–497.
4. Brino, L.; Urzhumtsev, A., Mousli, M.; Bronner, C.; Mitschler, A.; Oudet, P.; Moras, D. (2000). J. Biol. Chem.: 9468–9475.
5. Holdgate, G. A.; Tunnicliffe, A., Ward, W. H. J.; Weston, S. A.; Rosenbrock, G.; Barth, P. T.; Taylor, I. W. F.; Pauptit, R. A.; Timms, D. (1997). Biochemistry: 9663–9673.
6. Ronkin, S. M.; Badia, M., Bellon, S.; Grillot, A.-L.; Gross, C. H.; Grossman, T. H.; Mani, N.; Parsons, J. D.; Stamos, D.; Trudeau, M.; Wei, Y.; Charifson, P. S. (2010). Discovery of pyrazolthiazoles as novel and potent inhibitors of bacterial gyrase. Bioorg. Med. Chem. Lett.: 2828–2831.
7. Brvar, M.; Perdih, A.; Renko, M.; Anderluh, G.;Turk, D.; Solmajer, T. (2012). J. Med. Chem.: 6413-26
8. Glide version 6.3, Schrödinger, LLC, New York, NY, 2014
9. Steward, J. J. (1990), J. Comput.-Aided Mol.:4, 1-105.
10. SYBYL-X 2.1, Tripos International, 1699 South Hanley Rd., St. Louis, Missouri, 63144, USA

For more information see: